

## Wave-growth associated with turbulent spot in plane Poiseuille flow

By D. S. Henningson<sup>1</sup>, M. T. Landahl<sup>2</sup> and J. Kim<sup>3</sup>

A kinematic wave theory is used to investigate the cause of the rapid growth of waves observed at the wingtip of turbulent spot in plane Poiseuille flow. It is found that the qualitative behavior of the wave motions is well described by Landahl's breakdown criterion as the wave selection procedure. The predicted wave number, wave angle, and phase velocity are in agreement with those values obtained in a direct simulation.

### 1. Introduction

A localized disturbance in plane Poiseuille flow can develop into a turbulent spot if the Reynolds number ( $Re = U_{CL}h/\nu$ , where  $U_{CL}$  is the center line velocity and  $h$  is the half-channel height) is above about 1000. Experiments (Carlson et al. 1982; Alavyoon et al. 1986; Henningson & Alfredsson 1987) have shown that oblique waves develop around the spot as it propagates downstream. Henningson & Alfredsson (1987) observed the waves on the *wingtips*, i.e. the sides of the spot, consisted of the least stable Tollmien-Schlichting (T-S) mode. A recent numerical simulation of a Poiseuille flow spot (Henningson et al. 1987) shows that the wingtip wave-packet extends into the spot where the waves attain very high amplitude before they break down into turbulence. This indicates that the waves do play an important role in the rapid spanwise growth of the spot. In boundary layer spots (Chambers & Chambers 1983), however, waves are not seen to play such a role. This poses the following questions. Is the spreading of the two spots caused by different mechanisms? Are the waves just a passive response to disturbances in the surrounding laminar flow induced by the turbulence fluctuations? As a first step toward resolving these questions the present work addresses the cause of the rapid growth of the waves observed in Poiseuille spots. The related question of wave selection mechanism will also be considered.

### 2. Analysis

The wave pattern to be analyzed is shown in Fig. 1. Detailed descriptions of the computations can be found in Henningson et al. (1987). In what follows, all dimensional quantities are non-dimensionalized by the centerline velocity,  $U_{CL}$ ,

1 Aeronautical Research Institute of Sweden (FFA)

2 Massachusetts Institute of Technology

3 NASA Ames Research Center

and the channel half-width,  $h$ , and  $x$ ,  $y$ , and  $z$  denote the streamwise, vertical and spanwise directions, respectively. Fig. 1a shows a top view of  $\pm 0.01$  contours of the vertical velocity at the channel centerline. The front part of the spot has travelled a distance of about 200 from its generation point at this time,  $t = 258$ . Fig. 1b shows the modal shape of the waves for the first few amplitude maxima and Fig. 1c shows the corresponding spanwise amplitude variation at the centerline. The waves are seen to grow almost an order of magnitude as they propagate into the spot, while their modal shape still is essentially that of the simplest linear mode, i.e. the T-S wave. The calculations by Henningson et al. (1987) have shown that the phase speed in the streamwise direction of the waves are approximately 0.6, the absolute value of the wave number vector ( $k = \sqrt{\alpha^2 + \beta^2}$ ) about 1.8, and the angle ( $\phi$ ) between the wave number vector and the streamwise direction about  $-65^\circ$ . The velocity of the spot interface at the wingtip is approximately 0.7 in the streamwise direction and 0.12 in the spanwise direction. (The interface here is taken to be where the vertical velocity exceeds 0.02.)

A plausible explanation of the wave growth seen at the wingtip is interaction between the changing mean profile and the waves. If the time and spatial scales of the mean motion and the waves are widely separated, kinematic wave theory (Witham 1974) is appropriate to analyze their interaction. The starting point of the theory is a wave packet of the form,

$$ae^{i\theta}, \quad \theta = \alpha x + \beta z - \omega t$$

where  $a$ ,  $\alpha$ ,  $\beta$  and  $\omega$  are assumed to be slowly varying functions of space and time. The waves are assumed to have a known dispersion relation

$$\omega = W(\alpha, \beta, x, z, t)$$

which relates the variation of the angular frequency to the wavenumber vector components. Using the definition of the phase,  $\theta$ , and the dispersion relation, it can be shown (Witham 1974),

$$\begin{aligned} \frac{d\alpha}{dt} &= -\frac{\partial W}{\partial x} \\ \frac{d\beta}{dt} &= -\frac{\partial W}{\partial z} \\ \frac{d\omega}{dt} &= \frac{\partial W}{\partial t} \\ \frac{1}{A} \frac{dA}{dt} &= -\frac{\partial}{\partial x} \frac{\partial W}{\partial \alpha} - \frac{\partial}{\partial z} \frac{\partial W}{\partial \beta} \end{aligned}$$

along the rays defined by

$$\begin{aligned} \frac{dx}{dt} &= \frac{\partial W}{\partial \alpha} \\ \frac{dz}{dt} &= \frac{\partial W}{\partial \beta} \end{aligned}$$

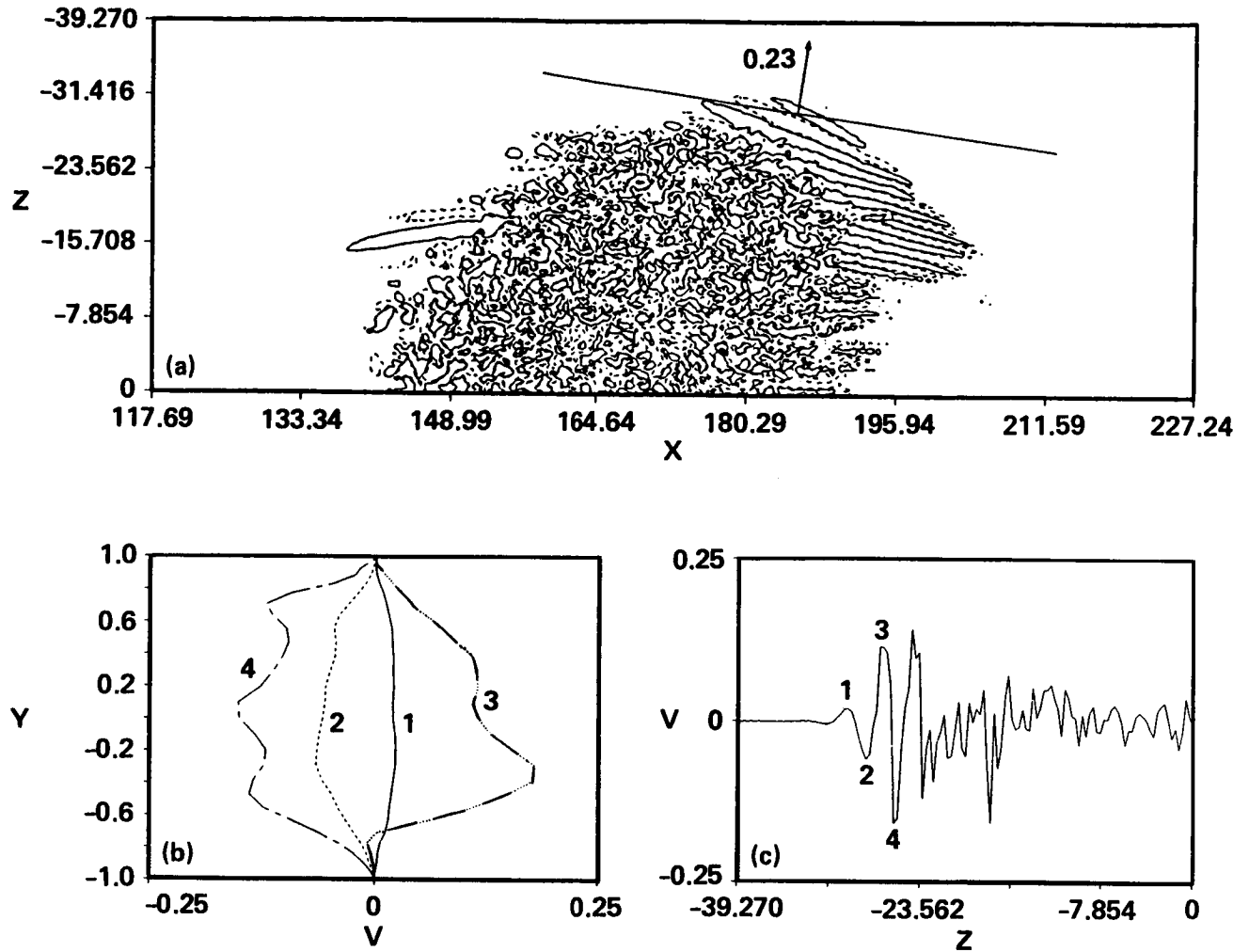


FIGURE 1. (a) A top view of  $\pm 0.01$  contours of the vertical velocity at the channel centerline:  $t=258$ ,  $Re=1500$ . (b) Profiles of the vertical velocity for the first few amplitude maxima: —,  $x=186$ ,  $z=-29.8$ ; ----,  $x=186$ ,  $z=-28.2$ ; ·····,  $x=186$ ,  $z=-26.7$ ; ---,  $x=186$ ,  $z=-25.5$ . (c) Spanwise variations of the vertical velocity at  $x=186$  and  $y=0$ .

where  $A$  is the wave action density, which is proportional to the square of the wave amplitude. The wave properties are seen to vary along the rays given by the group velocity,  $\vec{c}_g = (\partial W / \partial \alpha, \partial W / \partial \beta)$ . Landahl (1972) applied the above theory to oblique T-S waves riding on an inhomogeneity consisting of a larger scale locally two-dimensional wave. He was able to integrate the equation for the wave action density along a ray to yield

$$\frac{A}{A_0} = \frac{1}{c_{gn} - c_0}$$

where  $c_{gn}$  is the group velocity of the small scale oblique waves normal to the larger

two-dimensional wave, and  $c_0$  is the phase velocity of the two-dimensional wave. Notice when  $c_{gn}$  approaches  $c_0$  the wave amplitude will increase dramatically. This is a result of wave energy focusing. When the oblique waves approach the larger wave, their energy piles up on top of the large one since energy is constantly supplied by the incoming waves but no energy can leave, this results in an increase in the amplitude of the oblique waves.

As a first try we shall assume that the edge of the spot, where the waves are found, is locally two-dimensional, and we use the Landahl's breakdown criterion (Landahl 1972): i.e., we will examine if the group velocity of the wingtip waves, for any combination of wave numbers and frequency, is equal to the edge velocity at the wingtip. If the breakdown criterion is satisfied for a specific combination of  $\alpha$ ,  $\beta$  and  $\omega$ , then the wave will experience a rapid growth as it approaches the spot edge. Thus, this provides both a mechanism for growth and selection of the waves.

The dispersion relation for the T-S waves are found by solving an extended form of the Orr-Sommerfeld equation (see Henningson et al 1987). The appropriate mean velocity is

$$U(y) + W(y)\tan(\phi)$$

where  $U$  and  $W$  are the mean streamwise and spanwise velocity components, respectively.  $U$  and  $W$  are found by horizontal averaging and the required combination is fitted to a modified parabola

$$(1 - y^2)(c_0 + c_2y^2 + c_4y^4)$$

where  $c_0$ ,  $c_2$  and  $c_4$  are fitting constants. Profiles are fitted to the velocities seen in Fig. 2 using the appropriate wave angle (only  $\phi = 65^\circ$  is shown in the figure). They are obtained from the position indicated at the wingtip in Fig. 1a; the line in Fig. 1a indicates the tangent of the spot edge at this position and the arrow is in the direction of motion. Note that as the wave angle becomes large the departure of the fitted velocity profiles from the parabolic one become greater. This results from the inflectional character of the spanwise mean velocity, which have larger weight for higher wave angles.

When the Orr-Sommerfeld equation is solved, the dispersion relation found is usually complex. This requires a modification of the kinematic wave theory. Landahl (1972) used a simple approach, which involves adding a growth/decay rate term in the equation for the wave action density and the use of the real part of the dispersion relation when the group velocity is calculated. This requires small growth/decay rates and that the development of the wave packet is considered for short times only. Assuming this to be true the breakdown criterion is still valid (Landahl 1982). In the following we will thus use the real part of the dispersion relation in our effort to look for waves that satisfy the breakdown criterion.

### 3. Results and Discussion

Results from the solution of the Orr-Sommerfeld equation for the position indicated at the wingtip in Fig. 1a can be seen in Figs. 3-5. Contours of the group

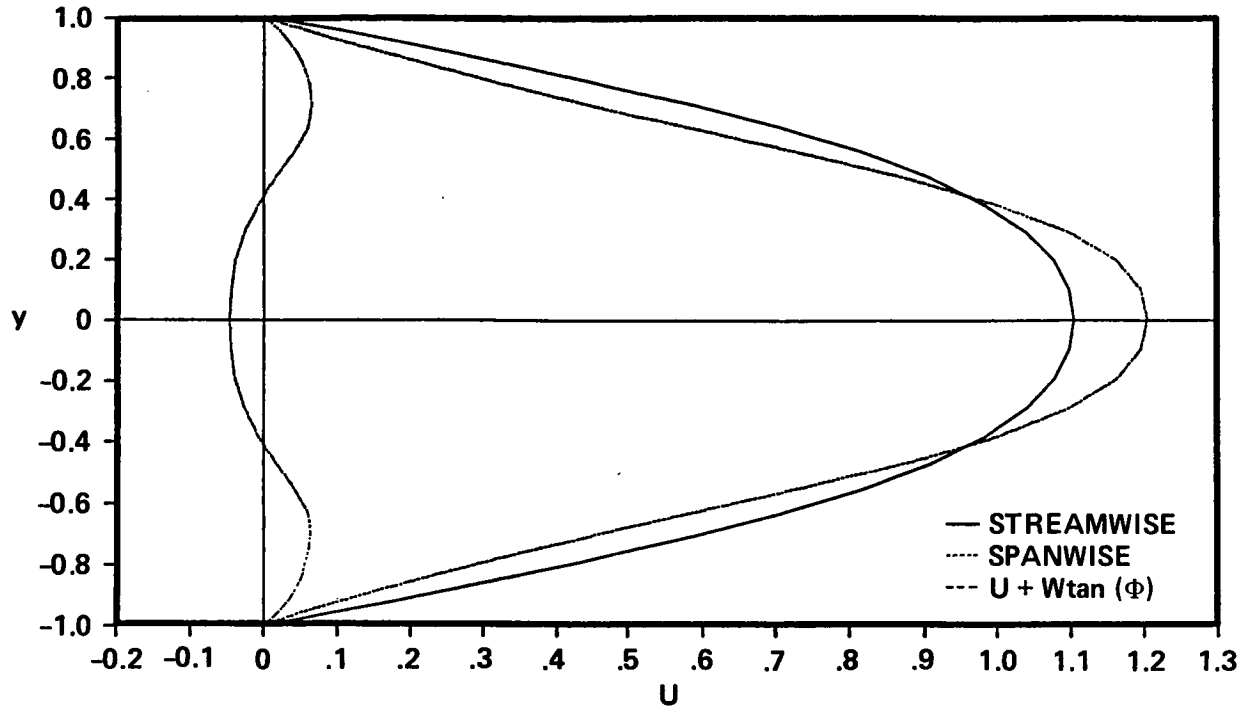


FIGURE 2. Mean velocity profiles at  $x=186$ ,  $z=-30$  and  $\phi = -65^\circ$ .

velocity perpendicular to the spot edge (i.e. in the direction of the arrow in Fig. 1a) are plotted as a function of  $k$  and  $\phi$  in Fig. 3. Figs. 4 and 5 show contours of the phase velocity in the streamwise direction and the imaginary part of the dispersion relation. Note that the group velocity attains its maximum of 0.25 for  $k = 1.0$  and  $\phi = 45^\circ$  (Fig. 3). The edge velocity at this location from the simulation was 0.23. The breakdown criterion is thus seen to be approximately fulfilled for  $k = 1.0$  and  $\phi = 45^\circ$ . This particular wave should grow to large amplitude at the wingtip of the spot. The waves actually observed has both higher wave number, wave angle and phase velocity. However, the waves are damped at this position (see Fig. 5) and only experience exponential growth for higher wave angles. Thus we might expect to find a wave that approximately fulfills the breakdown criterion and at the same time is growing exponentially. To find such a wave we follow the ridge going from the peak value in Fig. 3 up towards higher wave numbers. At around  $k=1.7$  and  $\phi = -65^\circ$ , the waves start to grow. This is close to the observed wave parameters. It should be noted here that this is an approximate analysis and that exact agreement cannot be expected. However, it is encouraging to see that the qualitative behavior of the normal group velocity, with its ridge going through the observed values, is able to select a wave using the breakdown criterion together with the requirement of exponential growth, and thus explain the observed wave motions. It should be an worthwhile effort in a future study to attack the full problem by tracing the wave rays into the spot and calculating the amplitude along them.

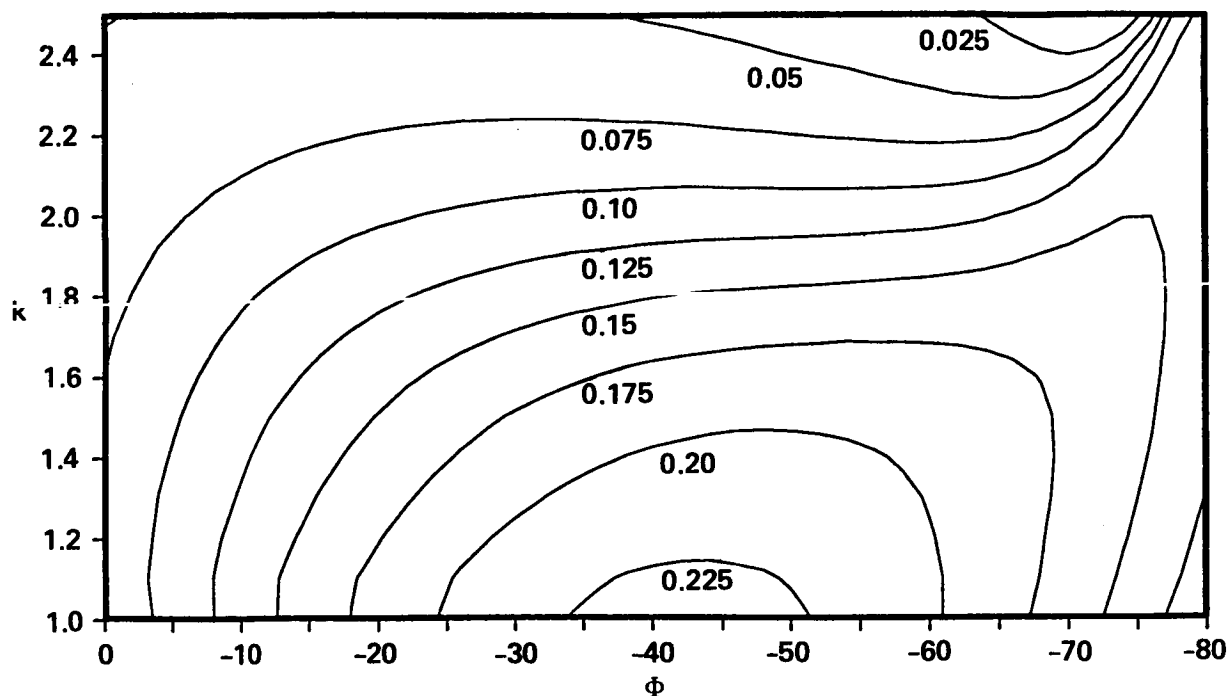


FIGURE 3. Contours of the group velocity perpendicular to the spot edge (i.e. in the direction of the arrow in Fig. 1a).

Finally, the picture that emerges from the present analysis is that the waves outside the spot are first generated by the moving turbulent disturbance, as discussed by for example Li & Widnall (1987), then they experience a growth by the wave energy focusing mechanism and the inflexional character of the effective mean velocity profile.

#### REFERENCES

- F. ALAVYOON, D. S. HENNINGSON, & P. H. ALFREDSSON 1986 Turbulent spots in plane Poiseuille flow - flow visualization. *Phys. Fluids* . **29**, 1328-1331.
- D. R. CARLSON, S. E. WIDNALL, & M. F. PEETERS 1982 A flow-visualization study of transition in plane Poiseuille flow. *J. Fluid Mech.* **121**, 487-505.
- F. W. CHAMBERS & A. S. W. CHAMBERS 1983 Turbulent spots, wave packets and growth. *Phys. Fluids*. **26**, 1160-1162.
- D. S. HENNINGSON & P. H. ALFREDSSON 1987 The wave structure of turbulent spots in plane Poiseuille flow. *J. Fluid Mech.* **178**, 405-421.
- D. S. HENNINGSON, P. R. SPALART & J. KIM 1987 Numerical simulations of turbulent spots in plane Poiseuille and boundary layer flows. *Phys. Fluids*. **30**, 2914-2917.
- M. T. LANDAHL 1972 Wave mechanics of breakdown. *J. Fluid Mech.* **56**, 775-802.

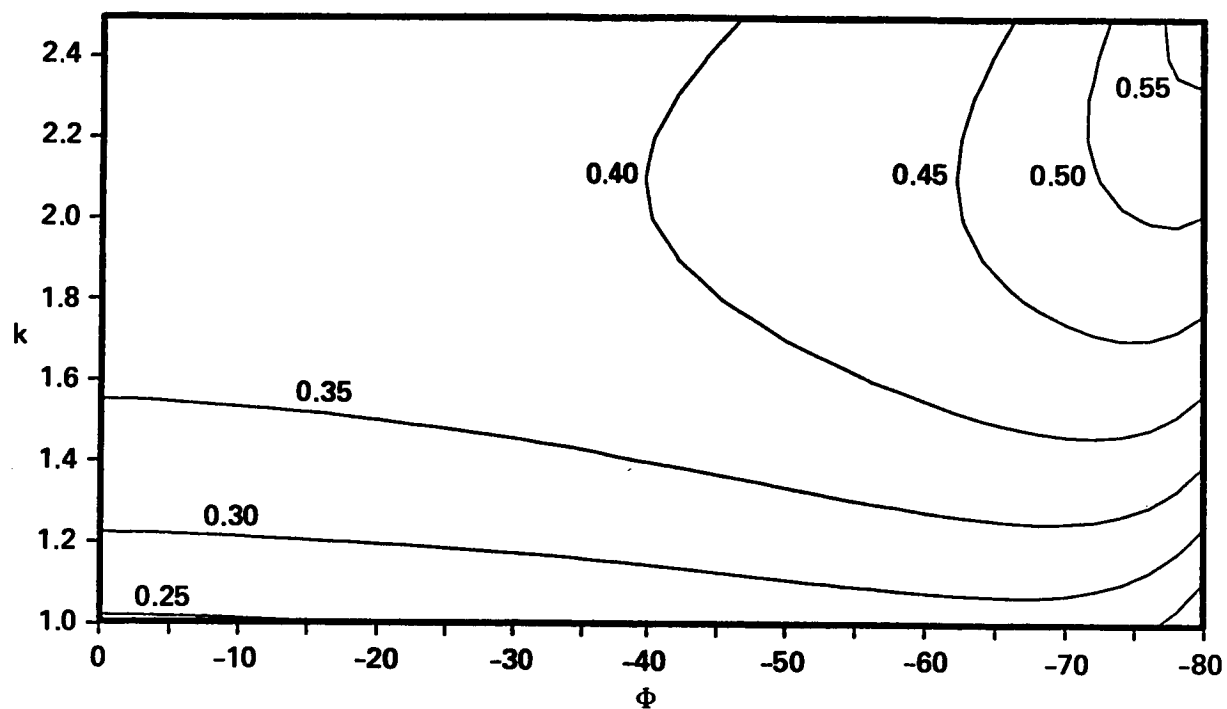


FIGURE 4. Contours of the phase velocity in the streamwise direction.

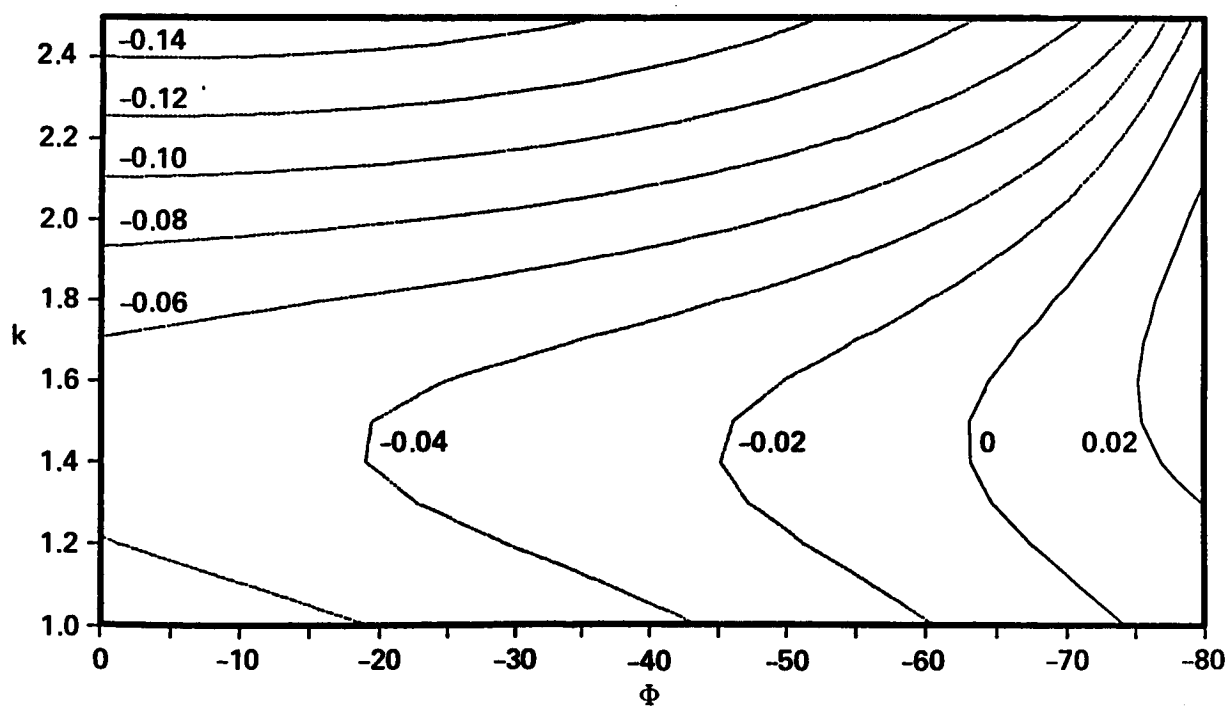


FIGURE 5. Contours of the imaginary part of the dispersion relation.

- M. T. LANDAHL 1982 The application of kinematic wave theory to wave trains and packets with small dissipation. *Phys. Fluids*. **25**, 1512-1516.
- F. LI & S. E. WIDNALL 1987 Wave patterns in plane Poiseuille flow created by concentrated disturbances. Submitted to *J. Fluid Mech.*
- G. B. WHITHAM 1974 Linear and nonlinear waves. Wiley.



## Appendix

During the summer program a special half day workshop on the role of coherent structures in turbulence modeling was organized by Prof. A. K. M. F. Hussain. The objective was to explore ideas in the use of the knowledge of organized structures in turbulence modeling.

Several participants were asked to make presentations, and five of these prepared written position papers that are included in this appendix. These statements appear as submitted by the authors. While these contain some interesting observations, the organizers of the Summer Program feel that no solution was put forward to the problem of incorporating the coherent structure research in Reynolds stress modeling. This reflects the great difficulty of achieving this integration. Perhaps the views expressed here will be helpful towards this end.